



ELSEVIER

Contents lists available at ScienceDirect

Microchemical Journal

journal homepage: [www.elsevier.com/locate/microc](http://www.elsevier.com/locate/microc)

# An improved ion chromatography system coupled with a melter for high-resolution ionic species reconstruction in Antarctic firn cores



Seokhyun Ro<sup>a,b</sup>, Soon Do Hur<sup>b</sup>, Sungmin Hong<sup>a</sup>, Chaewon Chang<sup>b</sup>, Jangil Moon<sup>b</sup>,  
Yeongcheol Han<sup>b</sup>, Seong Joon Jun<sup>b</sup>, Heejin Hwang<sup>b</sup>, Sang-bum Hong<sup>b,\*</sup>

<sup>a</sup> Department of Ocean Sciences, College of Natural Sciences, Inha University, Incheon 22212, South Korea

<sup>b</sup> Korea Polar Research Institute (KOPRI), 26 Songdomirae-ro, Yeosu-gu, Incheon 21990, South Korea

## ARTICLE INFO

### Keywords:

On-line multi-ion chromatography system  
Firn core melter  
Fluoride ion  
Methanesulfonate ion  
Styx Glacier  
Antarctica

## ABSTRACT

We improved an on-line multi-ion chromatography (IC) system combined with a custom firn core melter (IC-melter). Five anions ( $F^-$ ,  $CH_3SO_3^-$ ,  $Cl^-$ ,  $NO_3^-$ ,  $SO_4^{2-}$ ) and five cations ( $Na^+$ ,  $NH_4^+$ ,  $K^+$ ,  $Mg^{2+}$ ,  $Ca^{2+}$ ) are simultaneously determined every 1.3 min; high-resolution ion data, with a depth interval of approximately 1.8 cm, can thus be obtained from Antarctic firn cores using the IC-melter. The IC-melter provides a processing speed of 1.1–1.7 h per ~0.7–0.8 m firn core. The depth resolution was designed to capture seasonal variations of ions based on the accumulation rate of Styx Glacier (Northern Victoria Land, Antarctica), where a firn core used herein was obtained, and variations of the firn core density. The analytical conditions (eluent concentration and flow rate, run time, peak separation, and sensitivity) of the multi-IC system were optimized to achieve the research goals. Cations and anions were separated through 4-min isocratic elution ( $CH_3SO_3H$  eluent) and 5-min isocratic elution (KOH eluent), respectively. The isocratic elution method for anion analysis was selected, rather than the gradient elution method, due to the exceptionally low ionic strength of the meltwater and easy operation of the multi-IC system. All ionic species showed calibration curves with determinant coefficients  $> 0.997$ , standard errors of estimated values  $< 0.015$ , and relative standard deviation values  $< 4.17\%$  for anions and  $< 2.42\%$  for cations at levels of 5–25  $\mu g L^{-1}$ . The method detection limits (MDLs) for assessed ions were comparable to detection limits (DLs) previously reported for on-line IC-melter systems, except the limit of  $SO_4^{2-}$  ( $\sim 3.0 \mu g L^{-1}$ ). In particular, the MDLs of fluoride ion ( $F^-$ ) and methanesulfonate ion ( $CH_3SO_3^-$ ) were 0.03 and 0.3  $\mu g L^{-1}$ , respectively; these species were successfully measured in an Antarctic firn core for the first time, using the improved on-line IC-melter. The relative errors for ions other than  $Na^+$  and  $Cl^-$  were generally  $< 13.3\%$  at a level of approximately 50  $\mu g L^{-1}$ . The expanded measurement uncertainties ( $k = 2$  at the 95% confidence level) were  $\sim 0.13 \mu g L^{-1}$  and  $\sim 1.59 \mu g L^{-1}$  at levels of  $\sim 1.0 \mu g L^{-1}$  for  $F^-$  and  $\sim 5.0 \mu g L^{-1}$  for  $CH_3SO_3^-$ , respectively. The measured ions from parallel two firn core stick samples showed reproducibility values  $< 29.3\%$ . Pearson's  $r$  values between ions obtained from the IC-melter and conventional method were  $> 0.67$ . In this study, as an application of the IC-melter, high-resolution ion species data from the firn core (depth interval:  $\sim 20.11$ – $22.85$  m) are shortly presented.

## 1. Introduction

Ice cores from polar regions constitute an exceptionally reliable natural material for reconstruction of the past atmospheric environment, as they are formed through wet and dry deposition processes and its composition is related to atmospheric conditions at the time of deposition. Ice cores can preserve a valuable record of past climatic and environmental conditions without interference from human activities, providing high-resolution chemical profiles for comparison with materials such as ocean and lake sediments, tree rings, or cave stalagmites [1].

Ionic components in Antarctic ice cores are known to have originated primarily from the oceanic area surrounding Antarctica and partly from long-range transport of continental components. Therefore, variations in ion concentration are closely related to temporal changes in emission intensity from source areas (e.g., the Southern Ocean) and atmospheric transport to glaciers. For example, records of sea salt species (e.g.,  $Na^+$ ) have been used to reconstruct variations in sea ice concentration and atmospheric circulation. Biogenic sulfur compound (e.g., methanesulfonic acid ( $CH_3SO_3H$ ), hereafter referred to as MSA) is used as a proxy for primary productivity, sea ice area, and

\* Corresponding author.

E-mail address: [hong909@kopri.re.kr](mailto:hong909@kopri.re.kr) (S.-b. Hong).

<https://doi.org/10.1016/j.microc.2020.105377>

Received 31 March 2020; Received in revised form 30 June 2020; Accepted 4 August 2020

Available online 05 August 2020

0026-265X/ © 2020 Elsevier B.V. All rights reserved.

meteorological conditions. Non-sea-salt  $\text{SO}_4^{2-}$  (nss- $\text{SO}_4^{2-}$ ) and  $\text{F}^-$  are important components used for the detection of specific volcanic eruptions [2–7].

Ion chromatography (IC) and continuous flow analysis (CFA) systems have been widely used to measure the ionic species in ice cores, which are essential proxy data for ice core research programs. IC has been regarded as a valid method for the assessment of most ions (inorganic and organic anions and cations) in melted samples from ice cores [8,9]. IC offers the advantages of easy operation and sufficiently low sensitivity for ions of interest in ice cores. However, for the purpose of decontamination of ice cores, mechanical removal of contaminants and subcore sampling must be carefully conducted using a clean method that involves complicated and time-consuming procedures. CFA was developed to produce data at a high depth resolution of  $\leq 1$  cm from ice cores, drilled in glaciers with very low accumulation rates (approximately  $< 10$  cm snow  $\text{a}^{-1}$ ) [10]. Relatively simple ice core handling procedures are needed for CFA systems combined with ice core melters; however, only a few chemical species (e.g.,  $\text{Na}^+$ ,  $\text{NH}_4^+$ ,  $\text{Ca}^{2+}$ , and  $\text{NO}_3^-$ ) can be determined with the necessary sensitivity. As a result, to efficiently measure most ions in ice cores, an on-line IC measurement system combined with an ice core melter (IC-melter) has been progressively developed since 2000 [11,12]. High-resolution ion data have been successfully obtained with fast ion chromatography (FIC) or multi-IC systems connected to melters [13–15]. Furthermore, although the ionic species in meltwater samples obtained from the melter are not directly analyzed with the on-line IC measurement system, high-resolution sampling of meltwater using an automatic collection system followed by ion analysis using a standard IC system has been used as an alternative to the IC-melter to meet research goals [16–18].

Victoria Land in Antarctica is located in the western Ross Sea region, and is influenced by the Ross Sea, proximal polynyas (e.g., Ross Sea, McMurdo Sound, and Terra Nova Bay polynyas), several volcanoes (e.g., Mt. Erebus, Rittman, and Melbourne), and glaciers of the Transantarctic Chain, where katabatic winds are prevalent. Mountain areas of the Transantarctic Chain are a major source of dust deposited in the Ross Sea and glaciers of Victoria Land. Large-scale atmospheric circulation patterns (e.g., the Southern Annular Mode, El Niño Southern Oscillation, and Amundsen Sea Low) also affect the oceanic and atmospheric environment of the Ross Sea [19–23]. To reconstruct past environmental changes in this region (e.g., sea ice area, primary productivity, volcanic activity, and meteorological conditions) using ice cores from Victoria Land, therefore, it needs to investigate variations in concentrations of ionic species such as  $\text{CH}_3\text{SO}_3^-$ ,  $\text{F}^-$ , non-sea salt  $\text{Ca}^{2+}$  (nss- $\text{Ca}^{2+}$ ), and sea spray components. In particular,  $\text{F}^-$  is expected to give a supportive evidence in reconstruction of volcanic records from Antarctica and global volcanic events [7].

High-resolution ion data are critical for establishing an accurate chronology of ice cores and obtaining useful information regarding environmental changes that occurred over a short period (e.g., trends in maximum sea ice area from August to October, as well as irregular degassing from volcanoes in the Victoria Land region). For ion concentration variabilities affected by several emission sources (e.g.,  $\text{SO}_4^{2-}$  arising from biogenic emissions, sea spray, volcanic events, and sometimes continental dust), high-resolution stratigraphy can also help to clarify these complicated relationships.

Based on the advantages of the IC-melter reported in previous studies, thereby, an improved IC system was combined with a custom firm core melter [24] to provide high-resolution ionic profiles from Antarctic firm cores, enabling the first continuous high-resolution detection of  $\text{F}^-$  and  $\text{CH}_3\text{SO}_3^-$ . Thus far, these species have not been measured in proper sensitivity simultaneously by an on-line IC-melter, due to limits of the analytical method. Huber et al. [13] constructed an IC-melter system that could measure these ions in ice cores; however, it was unsuccessful to simultaneously detect  $\text{F}^-$  and  $\text{CH}_3\text{SO}_3^-$  in sub-ppb levels as well as relatively slow melting rate ( $\sim 0.45$  cm  $\text{min}^{-1}$ ) and low depth

resolution ( $\sim 4.0$  cm). Although our approach is similar to that described by Cole-Dai et al. [14], their method could measure only major anions (e.g.,  $\text{Cl}^-$ ,  $\text{NO}_3^-$ , and  $\text{SO}_4^{2-}$ ) and cations using CFA with a multi-IC system. Morganti et al. [17] reported an improved flow analysis IC method to measure  $\text{F}^-$ ,  $\text{CH}_3\text{SO}_3^-$ ,  $\text{Cl}^-$ ,  $\text{NO}_3^-$ , and  $\text{SO}_4^{2-}$  in the same run; however, their method involved measuring these species in discrete meltwater samples using a standard IC system.

The IC-melter was applied to a firm section (depth interval: 9.94–47.02 m) of a Styx ice core (hereafter referred to as Styx-M core) that had been drilled to a depth of 210.5 m in Styx Glacier (73°51.10'S, 163°41.22'E; 1623 m above sea level), Northern Victoria Land, Antarctica, as part of the Jang Bogo Station Ice Core Drilling Program in December 2014. First, stringent procedures were followed to obtain firm core stick samples [24]; meltwater from the firm core melter was then continuously injected into the on-line multi-IC system, which comprised three IC systems for anion analysis and three IC systems for cation analysis. The multi-IC system was optimized by installing IonPac AS15-5  $\mu\text{m}$  ( $3 \times 150$  mm) and CS12A-5  $\mu\text{m}$  ( $3 \times 150$  mm) analytical columns, and the performance (linearity, reproducibility, detection limit, and accuracy) of the IC system was investigated. A reproducibility test was carefully conducted using parallel firm core stick samples and ion data in discrete samples, prepared using conventional methods, were compared with those from the IC-melter constructed in this study. Finally, applications of high-resolution ion measurement by the IC-melter were suggested for the depth interval of 20.11–22.85 m (approximately 1922 to 1936 CE according to the firm densification model [29]) of the Styx-M core, such as identification of annual layers, seasonality of ions, and signals of volcanic activity.

## 2. Material and methods

### 2.1. Ion chromatography system and reagents

Analyses of anions ( $\text{F}^-$ ,  $\text{CH}_3\text{SO}_3^-$ ,  $\text{Cl}^-$ ,  $\text{NO}_3^-$ , and  $\text{SO}_4^{2-}$ ) and cations ( $\text{Na}^+$ ,  $\text{NH}_4^+$ ,  $\text{K}^+$ ,  $\text{Mg}^{2+}$ , and  $\text{Ca}^{2+}$ ) were performed using six IC detectors (ICS-5000, ICS-2100, ICS-2000 and two ICS-1100 instruments) from Thermo Fisher Scientific Dionex (Sunnyvale, CA, USA), combined with a firm core melter (Fig. 1).

The instrumental conditions of the IC sets are detailed in Table 1. A Thermo Fisher Scientific Dionex IonPac AS15-5  $\mu\text{m}$  ( $3 \times 150$  mm) analytical column and AERS-500 2-mm suppressor were installed on each IC instrument for anion analysis. A 5-min isocratic elution was performed for anion analysis using potassium hydroxide (KOH) as the eluent, which was generated from an eluent generation cartridge (EGC) (EGC-III KOH, Thermo Fisher Scientific Dionex). KOH eluent was selected rather than a buffer solution of  $\text{Na}_2\text{CO}_3$  and  $\text{NaHCO}_3$ , because it is better able to analyze traceable anions due to its low background conductivity ( $< 1$   $\mu\text{S cm}^{-1}$ ). Furthermore, the separation efficiency of anions is strongly affected by the purity of the KOH eluent; thus, KOH generated from the EGC was preferred, rather than KOH reagent. A Thermo Fisher Scientific Dionex IonPac CS12A-5  $\mu\text{m}$  ( $3 \times 150$  mm) analytical column and CERS-500 2-mm suppressor were installed on each IC instrument for cation analysis. A 4-min isocratic elution was performed for cation analysis on an ICS-5000 and two ICS-1100 systems using MSA eluent, which was generated from an MSA EGC (EGC-III MSA, Thermo Fisher Scientific Dionex) and a MSA reagent ( $\geq 99.0\%$ ) purchased from Sigma-Aldrich (St. Louis, MO, USA), respectively, because the two generation forms of MSA eluent showed no difference in separation efficiency of cations. Optimization of analytical conditions is described in detail in Section 3.2.

Chromeleon program (version 7) was utilized with the ICS-5000 system to combine six IC detectors with a six-way selection valve (Rheodyne, Cotati, CA, USA). This program controls various components of the multi-IC system; it also performs data acquisition and peak integration. In particular, the six-way selection valve and mode of the injection port (loading or injection) of the multi-IC system were

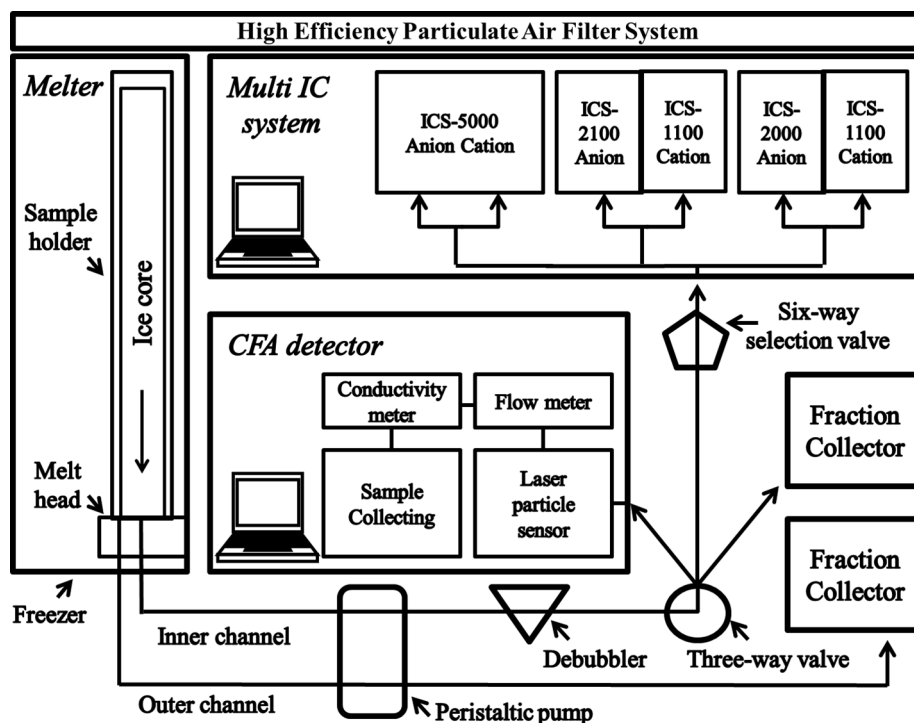


Fig. 1. Schematic diagram of our improved IC-melter system.

changed cyclically and simultaneously, in accordance with a programmed schedule.

Ultra-pure deionized water (DW) produced using a Milli-Q Integral Water Purification System (Merck Millipore; Burlington, MA, USA) was used to prepare all eluents and standard solutions. Mixed standard solutions for calibration were prepared by diluting a stock solution ( $\sim 1000 \text{ mg L}^{-1}$ ) of high-purity ( $> 99\%$ ) chemical reagents purchased from Sigma-Aldrich, which are listed in Table S1. To measure target ions in standard solutions using the IC instruments during the firm core melting process, direct injection of standard solutions into the selection valve was performed weekly. Chromatograms of the anions and cations in standard solutions and DW are presented in Fig. S1.

## 2.2. Firm core melting process

Continuous melting of firm core sections with density  $< 0.76 \text{ g cm}^{-3}$  was performed using a custom melter with a melt head of pure nickel. The design and material of the melt head and operation of the melter were described in detail by Hong et al. [24]. This improved melt head was designed to reduce the percolation effect of meltwater, which frequently occurs during processing of porous firm cores. The temperature of the heating block under the melt head was set to  $33 \pm 2 \text{ }^\circ\text{C}$  to obtain

the optimal melting rate for firm core processing. The melter was installed inside a freezer in a clean booth (ISO 5) situated within a clean room (ISO 6).

As a preparation process prior to melting of the firm core sample, a core sticks with a cross section of approximately  $3.2 \times 3.2 \text{ cm}$  was sawed from a cylindrical firm core (diameter  $\sim 10 \text{ cm}$ ), then carried to a clean booth (ISO 5) in the cold laboratory to minimize the possibility of contamination from the atmosphere. Dust particle number concentrations inside the clean booth were regularly detected using a particle counter (GT-521S, Met One Instruments, Grants Pass, OR, USA) to verify its cleanliness. Approximately  $0.6 \text{ cm}$  was chiseled from each end of the stick using pre-cleaned ceramic knives (Kyocera, Kyoto, Japan). An artificial ice core (a cross section of approximately  $\sim 3.2 \times 3.2 \text{ cm}$ ), prepared by freezing DW in a pre-cleaned jar [18], was placed at the bottom of the firm core stick for measurement of a procedural blank; it also allowed a constant melting rate of the firm core sample.

In firm core analysis, with an average melting rate of approximately  $\sim 1.3 \text{ cm min}^{-1}$ , meltwater ( $\sim 3.0 \text{ mL min}^{-1}$  of total sample volume) from the inner part of the firm core stick, which is considered the uncontaminated part, was passed through a glass debubbler [25] to remove air bubbles; it was then passed through a three-way valve that distributed the stream to CFA detectors ( $\sim 1.3 \text{ mL min}^{-1}$ ), including a

**Table 1**  
Instrumental conditions of our multi IC system.

System	Anion analysis			Cation analysis		
	ICS-5000	ICS-2100	ICS-2000	ICS-5000	ICS-1100	ICS-1100
Software	Chromleon 7.2 SR4			Chromleon 7.2 SR4		
Analytical column	IonPac AS15-5 $\mu\text{m}$ ( $3 \times 150 \text{ mm}$ )			IonPac CS12A-5 $\mu\text{m}$ ( $3 \times 150 \text{ mm}$ )		
Eluent	41 mM KOH	40 mM KOH	50 mM KOH	36 mM MSA		
Suppressor	AERS-500 2 mm			CERS-500 2 mm		
Flow Rate ( $\text{mL min}^{-1}$ )	0.89	0.89	1.0	0.6	0.6	0.57
Suppressor Current (mA)	91	89	124	64	64	61
Background Pressure (psi)	2220	2160	2340	2040	1880	1840
Background Conductivity ( $\mu\text{S cm}^{-1}$ )	0.320	0.110	0.120	0.280	0.570	0.380
Injection Volume	300 $\mu\text{L}$ per each injection			300 $\mu\text{L}$ per each injection		

laser particle counter (Abakus, Klotz, Unterhaugstett, Germany) and conductivity meter (829 Micro Flow Cell S/S\*, Amber Science Inc., Eugene, OR, USA) in series, and a six-way selection valve for loading the meltwater into the multi-IC system ( $\sim 0.9\text{--}1.0\text{ mL min}^{-1}$ ). The remaining sample stream from the debubbler was collected with a liquid fraction collector (Omnicoil Fraction Collector, Lambda, Brno, Czech Republic) ( $\sim 0.7\text{ mL min}^{-1}$ ) as an archive of the meltwater. The operation of the CFA detectors and data interpretation will be described in detail in a subsequent report.

### 2.3. Operation of on-line multi-IC system combined with a melter (IC-melter)

Before the on-line IC-melter began operation, the melter was thoroughly washed with DW until the conductivity of DW draining out from the inner zone of the melt head was below  $1\ \mu\text{S cm}^{-1}$ , indicating that the parts (connection tubes, glass debubbler, three-way valve, and six-way selection valve) from the melt head to the detectors were cleaned. Next, an instrumental blank of the multi-IC system was obtained by direct injection of DW into the six-way selection valve. Then, a system blank of the IC-melter was determined by injection of DW through the inner zone of the melt head into the multi-IC system. Based on these experimental procedures, blank values for the target ions and normal operations of the IC-melter were carefully checked out. If the blanks showed any measurable peaks for target ions, the melting process was conducted only after the melter had been cleaned. A procedural blank was obtained by measuring ions in meltwater from the artificial ice core. Chromatograms of the analyzed anions and cations from the instrumental blank, system blank, procedural blank, and melted samples from a firm section of the Styx-M core (e.g., 19.30–20.06 m in depth) are presented in Fig. S2.

The automatic operation of the IC-melter is described in Table S2. These loading and injection processes of the meltwater were cyclic until completion of firm core processing by the melter. Thus,  $\sim 1200\text{--}1300\ \mu\text{L}$  of a sample was loaded and divided into two injection sample loops of an IC set during ongoing analyses of samples that had already been loaded into other IC sets.

## 3. Results and discussion

### 3.1. Construction of the IC-melter

It has been suggested that high-resolution data of proxies, typically at least eight samples from a snow layer accumulated for one year, should be obtained to determine seasonal variations of environmental signals [26]. The proper depth resolution of proxy data in firm core samples can be estimated from the accumulation rate at the drilling site and density variations of firm cores with depth. The reported accumulation rate of Styx Glacier ranged from  $\sim 130$  to  $\sim 226\text{ kg m}^{-2}\text{ yr}^{-1}$  [27–30]. The density of the Styx-M core increases hyperbolically from  $\sim 350\text{ kg m}^{-3}$  in the surface snow layer to  $\sim 800\text{ kg m}^{-3}$  in the firm core section at a depth of 50 m [29]. In this study, the melting system was adjusted for use on firm core sections from below  $\sim 10$  m depth, where the density is generally  $> 500\text{ kg m}^{-3}$ , because the upper section was significantly more fragile and unsuitable for the melting process. A depth resolution of  $< 2.0\text{--}3.3\text{ cm}$  was needed to reconstruct at least eight ion data points within a snow layer for one year from firm core sections with densities of  $\sim 500\text{--}800\text{ kg m}^{-3}$ . Therefore, a depth resolution of  $\sim 2.0\text{ cm}$  of ion data was selected considering firm core section with the densities of  $\sim 800\text{ kg m}^{-3}$ , which is the thinnest part, and  $\sim 13, 11, 10,$  and  $9$  ion data points per year could be obtained from firm core section of  $\sim 10$  (density;  $\sim 500\text{ kg m}^{-3}$ ),  $\sim 20$  ( $\sim 600\text{ kg m}^{-3}$ ),  $\sim 30$  ( $\sim 700\text{ kg m}^{-3}$ ), and  $\sim 40$  ( $\sim 750\text{ kg m}^{-3}$ ) m depths, respectively.

The depth resolution of ion data from the IC-melter depends primarily on the performance of the IC system and the melting rate of the firm core. Because the melting rate of the firm core processed with the

melter was roughly  $\sim 1.0\text{--}1.5\text{ cm min}^{-1}$  at a melt head temperature of  $33 \pm 2\text{ }^\circ\text{C}$  [24], ion data from the IC system should be recorded every  $\sim 1.3\text{--}2.0\text{ min}$  to obtain a depth resolution of  $\sim 2.0\text{ cm}$ . However, separating multiple ionic species with proper peak resolution is difficult in the context of  $\sim 1.0\text{--}2.0\text{ min}$  analysis time using a single IC system (i.e., fast ion chromatography (FIC)) [7,9,11,15]. In particular,  $\text{F}^-$  and  $\text{CH}_3\text{SO}_3^-$ , which are the main target ions in the Styx-M core, should be quantitatively determined, but they have not yet been successfully analyzed using FIC systems. Moreover, the DLs of ions measured using the FIC system are generally higher than those of standard IC systems, which can use a pre-concentrator or large-volume sample loop. Therefore, the multi-IC system, which has a run time longer than that of a single FIC system, was expected to offer advantages in terms of obtaining appropriate peak separation and sensitivity for target ions in this study, although both systems can successfully provide high-resolution data for the target ions according to some research goals [14].

The multi-IC system was constructed by combining six IC detectors using a six-way selection valve (Fig. 1). This system was composed of three sets of IC detectors conducting simultaneous analysis of cations and anions. In particular, the six-way selection valve should be used to change the flow path of meltwater, which was critical for consecutive on-line measurements using the multi-IC system. Thus, the sample streams were distributed in sequence to three IC sets by the six-way selection valve.

Because ion determination in the meltwater was needed every  $\sim 1.3\text{--}2.0\text{ min}$  and three IC sets could be utilized for simultaneous analysis of anions and cations, the IC system required a run time of  $\sim 4.0\text{--}6.0\text{ min}$ . In this study, the melted sample was set to load into the multi-IC system with a run time of  $\sim 4.0\text{ min}$  at a flow rate of  $\sim 0.9\text{--}1.0\text{ mL min}^{-1}$  using a peristaltic pump (IP tubing pump, Ismatec, Zurich, Switzerland) during  $\sim 1.3\text{ min}$  ( $\sim 80\text{ s}$ ), which was the upper limit of the range needed to obtain a depth resolution near  $2.0\text{ cm}$  at a melting rate of  $1.5\text{ cm min}^{-1}$ .

For analysis of cations and anions, therefore,  $\sim 600\text{--}650\ \mu\text{L}$  of melted sample was loaded, which is  $\sim$  two-fold greater than the volume of the sample injection loop ( $\sim 300\ \mu\text{L}$ ). The on-line measurement system should be operated carefully to reduce the memory effect from the previous sample before the next sample is injected into the detector. In particular, the sample loops and connection tubes from the six-way selection valve to the injection port of the multi-IC system should be fully cleaned. However, no pre-cleaning step with DW was used before injection of the next sample; instead, the volume loaded into the sample loop was selected to flush out the loop and tubes prior to measurement of the next sample.

### 3.2. Optimization of analytical conditions in the multi-IC system

In this study, Thermo Fisher Scientific Dionex IonPac AS15-5  $\mu\text{m}$  ( $3 \times 150\text{ mm}$ ) and CS12A-5  $\mu\text{m}$  ( $3 \times 150\text{ mm}$ ) analytical columns, which have not been used in previous IC-melters [11–15], were selected to quantitatively analyze the target ions (in particular,  $\text{F}^-$  and  $\text{CH}_3\text{SO}_3^-$ ) with a run time of  $\sim 4.0\text{--}6.0\text{ min}$ .

It has been reported that the IonPac AS15 has an advantage in measurement of traceable inorganic anions and low molecular weight organic acids (short-chain carboxylate ions and  $\text{CH}_3\text{SO}_3^-$ ) in high-purity water matrices using a large injection loop for analysis at the  $\mu\text{g L}^{-1}$  level [31]. It was also expected that early-eluting anions, including  $\text{F}^-$ , from the water dip peak could be quantitatively separated due to their excellent retentions during flow through the analytical column, albeit relatively fast analytical conditions. Indeed, the IonPac AS15 ( $2 \times 240\text{ mm}$ ) has been successfully used in a standard IC system with  $200\text{--}500\ \mu\text{L}$  sample loops to determine  $\text{sub-}\mu\text{g L}^{-1}$  to  $\text{low-}\mu\text{g L}^{-1}$  levels of traceable ionic species in discrete melted samples of surface snow and ice cores in our laboratory since 2009 [18].

Cations could be determined more efficiently using CS12A-5  $\mu\text{m}$  ( $3 \times 150\text{ mm}$ ) with a total separation time of  $4.0\text{ min}$  based on the

previous result [32] (Fig. S3); therefore, we focused primarily on improving the analytical conditions for anion detection. Although the standard IC method generally emphasizes complete separation between neighboring peaks and the sensitivities of target ionic species, rather than total separation time, all of these factors should be appropriately considered due to the short running time (4.0–6.0 min) of the integrated IC system used in this study. Several anion measurement tests were conducted according to changes of eluent concentration (~40 to 90 mM KOH), eluent flow rate (~0.5 to 1.0 mL min<sup>-1</sup>) and column temperature (33–35 °C). The gradient elution method indicated that the separation time could be ~ 4.0–4.5 min with ~ 45 to 90 mM concentration and ~ 0.9 mL min<sup>-1</sup> flow rate of the KOH eluent, and a column temperature of 35 °C. The gradient was 45 mM KOH from 0.0 to 1.2 min, 45 to 90 mM KOH from 1.2 to 1.6 min, 90 mM KOH from 1.6 to 2.5 min, and 45 mM KOH from 2.6 to 4.0 min (Fig. S4a). The peak separation of target anions and change in run time according to the eluent flow rate are presented in Fig. S4b. The isocratic elution method also showed that NO<sub>3</sub><sup>-</sup> could be eluted within 5.0 min at ~ 40–41 mM concentration and ~ 0.92 mL min<sup>-1</sup> flow rate of the KOH eluent, and 35 °C column temperature. The KOH concentration of ~ 40–41 mM was selected to enhance separation of CO<sub>3</sub><sup>2-</sup> and SO<sub>4</sub><sup>2-</sup>, compared to ~ 45 mM KOH (Fig. S4c). Of the two elution methods tested for anion analysis, although the gradient elution method offered advantages of enhanced separation of neighboring peaks, the isocratic elution method was preferred due to the low ionic strength of the meltwater (generally < 10 μS cm<sup>-1</sup>) and easy adjustment of eluent conditions. When the eluent conditions of the gradient elution method were changed, the analytical condition of each analysis cycle of three IC sets for anion detection was required to be corrected (e.g., 10–15 analysis cycles per IC set, with a run time of 40–60 min).

To reduce the total separation time, the Thermo Fisher Scientific Dionex IonPac AG15-5 μm (3 × 30 mm) and IonPac CG12A-5 μm (3 × 30 mm) guard columns were not used, although a guard column is generally coupled with the analytical column in a standard IC system. The optimal conditions of concentrations and flow rates of eluents differed slightly for each IC instrument (Table 1) and they were continuously adjusted around these values during measurement period using on line IC-melter.

We intended to deploy a large sample loop rather than a pre-concentration column for the sake of simplicity of multi IC systems, low cost for installation, reproducibility of sample amount loaded, and routine melting process of firm core. Although use of a pre-concentration column can reduce the effects of the water dip at the beginning of the chromatograms, compared with a large sample loop, the quantity of meltwater loaded should be carefully controlled to be constant when a pre-concentration column is applied [12,17,31] and the concentration efficiency of ions might be also affected by ionic composition. The sample loop volume was set to ~ 300 μL to ensure appropriate detection limits for ions of interest in this study after sequential testing of 75, 200, and 300 μL. The sample volume loaded can affect separation of several anions with similar retention time and also contribute to the size of system water dip peak. In particular, short-chain organic acids (e.g., acetic and formic acid) in snow and ice cores from polar regions can affect the quantitative analysis of F<sup>-</sup> if they are not properly separated. As the injection volume increases (75 to 300 μL), the void volume increased and thus run time of ions was steadily delayed. The results showed that the peak from F<sup>-</sup> is properly separated from the water dip and the peak resolutions (R<sub>s</sub>) of F<sup>-</sup> and organic anions (organic anions and CH<sub>3</sub>SO<sub>3</sub><sup>-</sup>) are ~ 1.2–1.4 (~1.5–1.7), which means that they can be measured quantitatively (Figs. S1 and S2).

The overlap between peaks of unknown ions and target ions should be refined to obtain valid concentrations of target ions. Fig. S5 illustrates the separation between such organic acids and F<sup>-</sup> after the water dip and that other ions (i.e., NO<sub>2</sub><sup>-</sup>, Br<sup>-</sup>, and PO<sub>4</sub><sup>2-</sup>) did not overlap with the target ions in this study. Interestingly, NO<sub>3</sub><sup>-</sup> was eluted at ~4.6 min; therefore, NO<sub>3</sub><sup>-</sup> from previous sample was eluted

immediately before the water dip of the next sample. For standard IC systems, it is generally recommended that analytes in an injected sample are eluted until the end of each analysis cycle; the following sample should then be injected after the conductivity of eluent completely returns to initial background level of analysis cycle. However, in this study, we could inject samples at intervals of 1.3 min (80 s) for consecutive analysis of multi-IC system and thus samples were injected every 4 min for each IC system before NO<sub>3</sub><sup>-</sup> was not eluted. This could be achieved because the isocratic elution method provides constant concentration level of eluent during the analysis cycle. Because water, which has a very low dissociation constant (1.0 × 10<sup>-14</sup> mol<sup>2</sup> L<sup>-2</sup>), should be eluted first through the IC analytical column after injection, NO<sub>3</sub><sup>-</sup> from the previous sample (eluted before the water dip peak of a sample) was rarely mixed with other ions in that sample. If any unknown components other than NO<sub>3</sub><sup>-</sup> from the previous sample were eluted after the water dip peak of a sample, they could have caused positive interference for the quantitation of target ions in that sample. Although phosphate (PO<sub>4</sub><sup>3-</sup>) was eluted approximately 6.5 min after NO<sub>3</sub><sup>-</sup> elution using the isocratic elution method, its effect was expected to be very small, as it has rarely been detected in snow and ice cores from Antarctica. Furthermore, the run time of PO<sub>4</sub><sup>3-</sup> nearly overlapped with a CO<sub>3</sub><sup>2-</sup> peak of the next sample (Fig. S5).

### 3.3. Performance of the on-line multi-IC system

Calibration parameters such as concentration range, regression equation, coefficient of determination (r<sup>2</sup>), standard error of the estimate, and relative standard deviation are listed in Table 2. All ionic species had r<sup>2</sup> values > 0.997 and standard error of the estimate values < 0.015. The relative standard deviation values were < 4.17% for anions and < 2.42% for cations at levels of 5–25 μg L<sup>-1</sup>. These results indicated that the values estimated from the regression equations were reliable and that measurement results from the multi-IC system did not vary over a short time period.

Method detection limits (MDLs) were calculated to investigate the sensitivities of ions measured under analytical conditions of the IC sets, then compared with those from previous studies (Table 3). Most ions showed comparable MDLs with DLs of other studies, except SO<sub>4</sub><sup>2-</sup>. SO<sub>4</sub><sup>2-</sup> showed the highest MDLs (~3.0 μg L<sup>-1</sup>) due to a lack of baseline separation of the CO<sub>3</sub><sup>2-</sup> and SO<sub>4</sub><sup>2-</sup> peaks (Fig. S1a). As a systematic peak of the IC system using KOH eluent, the CO<sub>3</sub><sup>2-</sup> peak rarely influences SO<sub>4</sub><sup>2-</sup> quantitation in the standard IC method, which has peak resolution (R<sub>s</sub>) of ~ 1.2–1.4 between CO<sub>3</sub><sup>2-</sup> and SO<sub>4</sub><sup>2-</sup> [18]. However, these species could not be properly separated using the isocratic elution method applied to the multi-IC system in this study. Therefore, a carbonate removal device (CRD) (CRD-200 4 mm, Thermo Fisher Scientific Dionex) was tested to reduce the CO<sub>3</sub><sup>2-</sup> peak area. The response (~0.2–0.3 μS at peak height) of CO<sub>3</sub><sup>2-</sup> in the multi-IC system using the CRD was ~ 20–30% of that (~0.7–0.8 μS) without the CRD, indicating enhanced separation of the CO<sub>3</sub><sup>2-</sup> and SO<sub>4</sub><sup>2-</sup> peaks (Fig. S1b) and improved sensitivity for SO<sub>4</sub><sup>2-</sup>. The MDL of SO<sub>4</sub><sup>2-</sup> in the IC system with a CRD was ~ 1.1 μg L<sup>-1</sup>, which is approximately one-third of the MDL of the IC system without a CRD (~3.0 μg L<sup>-1</sup>).

Table S3 lists the concentration ranges of target ions measured using the standard IC method in discrete samples of a firm core (hereafter referred to as Styx-B core) and a snow pit sample collected near the drilling site of the Styx-M core in December 2014. Because the concentrations of ions in the real sample from Styx Glacier are generally several fold greater than the MDLs of those ions, the IC-melter was expected to successfully determine not only SO<sub>4</sub><sup>2-</sup>, but also other ions in the Styx-M core. In particular, the concentrations of SO<sub>4</sub><sup>2-</sup> in the Styx-B core and snow pit ranged from 13.38 to 2506.58 μg L<sup>-1</sup> (average: 91.63 μg L<sup>-1</sup>) and 14.08 to 1732.80 μg L<sup>-1</sup> (178.20 μg L<sup>-1</sup>), respectively (Table S3). Therefore, in this study, SO<sub>4</sub><sup>2-</sup> in most melted samples from the firm core section of the Styx-M core was determined using the multi-IC system without CRD. With this analytical technique,

**Table 2**  
Calibration parameters of our multi IC system.

Species	Concentration range <sup>a</sup> ( $\mu\text{g L}^{-1}$ )	Regression		$r^2$	S.E.E. <sup>b</sup>	R.S.D. <sup>c</sup> (%)
		Slope	Intercept			
F <sup>-</sup>	0.1–5	0.004–0.005	–0.002–0.001	0.999–1.000	< 0.002	1.34
CH <sub>3</sub> SO <sub>3</sub> <sup>-</sup>	5–50	0.001	–0.001–0.000	0.997–0.999	< 0.004	2.03
Cl <sup>-</sup>	25–500	0.004	–0.025–0.010	1.000	< 0.008	1.46
SO <sub>4</sub> <sup>2-</sup>	25–500	0.003	–0.033–0.006	1.000	< 0.009	3.29
NO <sub>3</sub> <sup>-</sup>	0.5–25	0.001–0.002	–0.004–0.002	1.000	< 0.005	4.17
Na <sup>+</sup>	10–200	0.005	–0.006–0.002	1.000	< 0.001	1.30
NH <sub>4</sub> <sup>+</sup>	0.25–12.5	0.005–0.006	0.004–0.007	0.998	< 0.015	1.44
K <sup>+</sup>	0.5–25	0.003	–0.002–0.001	0.998–0.999	< 0.003	1.47
Mg <sup>2+</sup>	12.5–250	0.006–0.009	–0.015–0.032	1.000	< 0.010	2.30
Ca <sup>2+</sup>	0.5–25	0.006	–0.005–0.002	0.998–1.000	< 0.003	2.42

<sup>a</sup> It indicates the normal concentration range for calibration of most samples. The high concentrations of ions measured in a few samples were determined by calibration curves calculated with high concentrations of standard materials.

<sup>b</sup> Standard error of the estimate.

<sup>c</sup> Relative standard deviation was calculated as the following: Standard deviation/Mean  $\times$  100 (%) of 12 replicates of a 5  $\mu\text{g L}^{-1}$  (F<sup>-</sup>), 10  $\mu\text{g L}^{-1}$  (Na<sup>+</sup>), 12.5  $\mu\text{g L}^{-1}$  (NH<sub>4</sub><sup>+</sup>, Mg<sup>2+</sup>) and 25  $\mu\text{g L}^{-1}$  (CH<sub>3</sub>SO<sub>3</sub><sup>-</sup>, Cl<sup>-</sup>, SO<sub>4</sub><sup>2-</sup>, NO<sub>3</sub><sup>-</sup>, K<sup>+</sup>, Ca<sup>2+</sup>) standard solution.

**Table 3**

Intercomparison of detection limits of chemical components among our IC-melter system and other on-line IC systems combined with melter (unit of concentration:  $\mu\text{g L}^{-1}$ ).

Species	This study	[13] <sup>c</sup>	[14] <sup>d</sup>	[15] <sup>e</sup>
	MDL <sup>a</sup>	LOD	MDL	LOD
F <sup>-</sup>	~0.03	0.1		
CH <sub>3</sub> SO <sub>3</sub> <sup>-</sup>	~0.3	1.2		
Cl <sup>-</sup>	~0.09	0.1	0.4	5.0
SO <sub>4</sub> <sup>2-</sup>	~3.0–1.1 <sup>b</sup>	1.0	0.07	2.0–4.0
NO <sub>3</sub> <sup>-</sup>	~0.6	0.5	0.02	2.0
Na <sup>+</sup>	~0.08	0.8	0.04	
NH <sub>4</sub> <sup>+</sup>	~0.1	1.4	0.06	
K <sup>+</sup>	~0.05	1.8	0.7	
Mg <sup>2+</sup>	~0.02	1.1	0.004	
Ca <sup>2+</sup>	~0.06	2.6	0.004	

<sup>a</sup> Method detection limits (MDLs) of ions detected by multi IC system without carbonate removal device (CRD) were calculated as multiplying the Student's t-value for a single-tailed 99th percentile t statistic and a standard deviation estimate with the degrees of freedom of the number of replicates and the standard deviation of 7 replicates of a 0.1  $\mu\text{g L}^{-1}$  (F<sup>-</sup>), 0.2  $\mu\text{g L}^{-1}$  (Na<sup>+</sup>), 0.25  $\mu\text{g L}^{-1}$  (NH<sub>4</sub><sup>+</sup>, Mg<sup>2+</sup>), 0.5  $\mu\text{g L}^{-1}$  (Cl<sup>-</sup>, NO<sub>3</sub><sup>-</sup>, K<sup>+</sup>, Ca<sup>2+</sup>), 5  $\mu\text{g L}^{-1}$  (CH<sub>3</sub>SO<sub>3</sub><sup>-</sup>) and 25  $\mu\text{g L}^{-1}$  (SO<sub>4</sub><sup>2-</sup>) standard solution. Only the highest MDL values among the values from the three IC sets are presented here.

<sup>b</sup> MDL of SO<sub>4</sub><sup>2-</sup> detected by multi IC system with CRD were calculated as multiplying the Student's t-value for a single-tailed 99th percentile t statistic and a standard deviation estimate with the degrees of freedom of the number of replicates and the standard deviation of 7 replicates of a 5  $\mu\text{g L}^{-1}$  (SO<sub>4</sub><sup>2-</sup>) standard solution. Only the highest MDL values among the values from three IC sets are presented here.

<sup>c</sup> Limit of detections (LODs) are defined as 10 blank values of ultra-pure water producing a signal-to-noise of 3.

<sup>d</sup> MDLs were determined using the root mean square error method.

<sup>e</sup> LODs were calculated as the mean plus three times the standard deviation of the signal of 10 replicate injections of a blank solution divided by the sensitivity.

only 0.6%, 1.8%, 0.2%, 0.3%, and 0.1% of F<sup>-</sup>, CH<sub>3</sub>SO<sub>3</sub><sup>-</sup>, SO<sub>4</sub><sup>2-</sup>, NO<sub>3</sub><sup>-</sup>, and Mg<sup>2+</sup> samples, respectively, were not quantitatively detected due to concentrations below their MDLs.

In contrast, the NH<sub>4</sub><sup>+</sup> concentration was strongly influenced by the abundance of Na<sup>+</sup> (Fig. S2). Although the MDL of NH<sub>4</sub><sup>+</sup> is approximately 0.1  $\mu\text{g L}^{-1}$  for standard solution containing similar levels (~0.20–0.25  $\mu\text{g L}^{-1}$ ) of Na<sup>+</sup> and NH<sub>4</sub><sup>+</sup>, ~40% of NH<sub>4</sub><sup>+</sup> samples could not be quantitatively determined due to values below the MDL or the presence of overlapped peaks between Na<sup>+</sup> and NH<sub>4</sub><sup>+</sup>. In particular,

large Na<sup>+</sup> peaks frequently caused considerable uncertainty in the calculation of NH<sub>4</sub><sup>+</sup> peak area. This uncertainty is a limitation of the analytical conditions (e.g., run time of 4 min) used for cation analysis with the CS12A-5  $\mu\text{m}$  (3  $\times$  150 mm) column. Application of a cation analysis column with higher capacity (e.g., CS16A) might improve quantitative determination of NH<sub>4</sub><sup>+</sup> in samples with higher concentration ratios of Na<sup>+</sup> to NH<sub>4</sub><sup>+</sup> (e.g., ratios of approximately 75 and 340 based on the median and average concentrations, respectively, of Na<sup>+</sup> and NH<sub>4</sub><sup>+</sup> in surface snow on Styx Glacier).

The relative error values of ions were calculated to estimate the accuracy of ion concentrations measured by the multi-IC system (Table S4). Combined and diluted solutions (~50  $\mu\text{g L}^{-1}$ , except for Na<sup>+</sup> and Cl<sup>-</sup>) of reference materials prepared from high-purity chemical reagents in the laboratory (Table S5) were utilized. Relative error values of Na<sup>+</sup> (114.7  $\mu\text{g L}^{-1}$ ) and Cl<sup>-</sup> (378.6  $\mu\text{g L}^{-1}$ ) were –0.3487% and 1.532%; all others ranged from –7.51% (CH<sub>3</sub>SO<sub>3</sub><sup>-</sup>) to 3.05% (NO<sub>3</sub><sup>-</sup>) for anions and –13.3% (Ca<sup>2+</sup>) to –2.40% (K<sup>+</sup>) for cations. Calculated relative error levels < 13.3% indicated that the concentrations of chemical components measured with our IC system were acceptable. Because the average (median) values of F<sup>-</sup> and CH<sub>3</sub>SO<sub>3</sub><sup>-</sup> in the Styx-M core were ~1.2 (~0.46) and ~7.8 (~4.5)  $\mu\text{g L}^{-1}$ , respectively, measurement uncertainties of F<sup>-</sup> and CH<sub>3</sub>SO<sub>3</sub><sup>-</sup>, which were firstly determined with the on-line IC method used in this study, were estimated at these levels based on the major contributors of uncertainty (Supplementary Material S1). Preparation of standard solutions, determination with the calibration curve, and repeatability of the on-line measurement system might be possible major sources of measurement errors. We suggested standard uncertainty values for these factors likely to contribute measurement uncertainties in Tables S6 and S7. The expanded measurement uncertainties ( $k = 2$  at the 95% confidence level) were ~0.13  $\mu\text{g L}^{-1}$  and ~1.60  $\mu\text{g L}^{-1}$  at levels of ~1.0  $\mu\text{g L}^{-1}$  F<sup>-</sup> and ~5.0  $\mu\text{g L}^{-1}$  CH<sub>3</sub>SO<sub>3</sub><sup>-</sup>, respectively.

### 3.4. Performance of the IC-melter

Depth resolution of ion data and efficient processing of the ice core are regarded as important performance indicators for the on-line IC-melter. The depth resolution of ions measured by the IC-melter averaged approximately 1.8 cm with a sample loading time of ~1.3 min and melting rate of ~1.3 cm min<sup>-1</sup>. These values represented the actual depth resolution of ionic species, as the sample loading time was greater than the mixing time (~53 s) of melted samples, calculated using the method of Cole-Dai et al. [14], in the tube after passing through the debubbler. In these instances, the mixing of meltwater from the melt head to the debubbler was assumed to be limited due to the

presence of air bubbles separating the melted samples while they flowed through the drain tube of the melt head.

Processing by the IC-melter typically required approximately  $\sim 0.6$ – $1.2$  h per  $\sim 0.7$ – $0.8$  m of firn core stick sample, depending mainly on the melting rate ( $\sim 1.0$ – $1.5$  cm min<sup>-1</sup>) of the firn core. Additional time of up to  $\sim 1.1$ – $1.7$  h was generally spent operating the IC-melter due to extra preparation processes including cleaning procedures for some parts of the melter (i.e., melt head, connection tubes, debubbler, and three-way valve) with DW and analysis of system blanks.

Multiple signals from various detectors used to measure several proxies in the meltwater should be coregistered to allow investigation of the relationships of these proxies within a depth interval and their concentration variabilities over the same period. Electrical conductivities (ECs) were calculated theoretically from equivalent concentrations of measured ionic species and compared with the ECs measured by the on-line conductivity meter (Fig. S6). Because hydrogen ion (H<sup>+</sup>) in the meltwater was not measured directly in this study, its abundance was calculated from the difference of the sums of equivalent concentrations of anions and cations, based on the electroneutrality of meltwater. Fig. S6 indicates that EC values from the on-line conductivity meter were generally larger than those from the theoretically one and EC values from the two methods corresponded very well at the same firn core depth. Although these values were not theoretically identical due to a lack of anion (e.g., short-chain organic acids) measurement by the multi-IC system, which caused miscalculation of the concentration of hydrogen ions that contributed to the EC of melted samples, signals from CFA detectors (e.g., the on-line dust monitor and conductivity meter) could be coregistered with the ion data measured using the multi-IC system.

To determine the reliability of the ion concentrations measured by the IC-melter, a reproducibility test using parallel firn core stick samples collected at the same depth intervals and comparison with ion data in discrete samples prepared using conventional method were carefully conducted. Only ions other than NH<sub>4</sub><sup>+</sup> were considered, because the NH<sub>4</sub><sup>+</sup> concentration was very low in the firn core for most of the depth interval of interest, which would cause large uncertainties in the measured results as described in Section 3.3.

The reproducibility of IC-meter was tested by comparing concentrations of ions from a section of the Styx-M core, 20.89–21.64 m in depth, and a sample of the original section turned upside-down (Fig. 2a and Table S8). Fig. 2a shows that the concentrations of ions in the two samples corresponded well at each depth interval, with few exceptions. This result supported the validity of ion measurements from the IC-melter and the homogeneity of ions in adjacent snow layers. At approximately 21.40 m in depth, where firn core sticks were broken and thus liable to be affected by contaminants, the concentrations of most ionic species exhibited greater discrepancies than at other depth intervals. The measured sea spray components (i.e., Na<sup>+</sup>, Cl<sup>-</sup>, K<sup>+</sup>, Mg<sup>2+</sup>, and Ca<sup>2+</sup>) and NO<sub>3</sub><sup>-</sup> of the original sample showed good reproducibility compared to the upside-down sample; all components differed by  $< \sim 9.9\%$ , except for Ca<sup>2+</sup> ( $\sim 29.3\%$ ). CH<sub>3</sub>SO<sub>3</sub><sup>-</sup>, SO<sub>4</sub><sup>2-</sup>, and F<sup>-</sup> also showed moderate agreement of  $\sim 13.2\%$ ,  $\sim 10.8\%$ , and  $\sim 23.2\%$ , respectively.

Ion data measured by the IC-melter from a firn core section 19.30–20.07 m in depth were also compared with those obtained from the standard IC method [18] using discrete samples (depth resolution:  $\sim 4.0$ – $5.8$  cm) that had been processed by the conventional chiseling technique, which is described in Supplementary Material S2 (Fig. 2b). Fig. S7 shows that concentrations of ions from the third layer (innermost) were generally lower than those from the second and first layers (outermost); this indicates the importance of removing the outer layers of firn core sticks, which are sensitive to contamination during the preparation procedures. Among ions, the ratios ( $\sim 2.3$ – $6.0$ ) of NO<sub>3</sub><sup>-</sup>, K<sup>+</sup>, and Ca<sup>2+</sup> concentrations in the first layer samples with respect to concentrations in third layer samples were higher than those ( $< 1.5$ ) of

other ions. In particular, the concentration ratio of Ca<sup>2+</sup> ( $\sim 6.0$ ) indicated its likelihood of contamination during firn core preparation, despite meticulous control measures.

Fig. 2b shows that the concentration variabilities of the two methods generally corresponded, indicating the effectiveness of ion measurement using the IC-melter. The calculated Pearson's  $r$  values of anions from the two methods were 0.85, 0.87, 0.86, 0.83, and 0.67 for F<sup>-</sup>, CH<sub>3</sub>SO<sub>3</sub><sup>-</sup>, Cl<sup>-</sup>, SO<sub>4</sub><sup>2-</sup>, and NO<sub>3</sub><sup>-</sup>, respectively. Among cations, Na<sup>+</sup> and Mg<sup>2+</sup> showed Pearson's  $r$  values  $> 0.76$ , while those for K<sup>+</sup> (0.60) and Ca<sup>2+</sup> (0.30) were lower. The K<sup>+</sup> and Ca<sup>2+</sup> concentrations obtained from the conventional method were noticeably higher than those from the IC-melter in the top and bottom sections of the firn core sample; Pearson's  $r$  values increased to 0.82 and 0.71, respectively, after those sections had been removed. These indicated that K<sup>+</sup> and Ca<sup>2+</sup> were more sensitive to contamination in the top and bottom sections of firn core samples during sample preparation for the conventional method.

Although the concentration variabilities of ions in the firn core in Fig. 2b were related to temporal changes of past environmental conditions in this region, they also may have been influenced by the depth resolution of ion data reconstructed, as well as their feasibilities of contamination during firn core preparation. As expected, ion data obtained from the IC-melter clearly showed concentration variations over short depth intervals; the amplitude of ion concentration variability is generally greater than that of the conventional method. Ion data from the conventional method showed a smoothing effect due to the lower depth resolution of this method.

According to previous studies, ion data from the on-line IC-melter might be more accurate than those obtained from the conventional method, because samples melted by the melter are less likely to be influenced by contaminants [12,14,15]. In particular, measurement of some cations using the conventional method might be sensitively affected by probable contamination sources during sample preparation. Cole-Dai et al. [14] reported higher concentrations of K<sup>+</sup>, Mg<sup>2+</sup>, and Ca<sup>2+</sup> in discretely prepared samples than in samples prepared using the on-line IC-melter method; they suggested incomplete cleaning of sample containers as a possible source of contamination for these ions. However, Fig. 2b presents no consistent higher concentrations in discrete samples processed using the conventional method; similar concentrations were observed except in the top and bottom sections of the firn core, although Ca<sup>2+</sup> concentrations of discrete samples were clearly higher at  $\sim 19.45$ – $19.62$  m depth. Among anions, CH<sub>3</sub>SO<sub>3</sub><sup>-</sup> and NO<sub>3</sub><sup>-</sup> in discrete samples also exhibited higher concentrations at  $\sim 19.45$ – $19.62$  m depth; these trends were presumed to be more obvious at depth intervals with low concentrations. Comparison of ion data obtained from these two methods indicated that the relationship between concentrations of ions measured by the two methods may differ in accordance with experimental conditions, such as the cleanliness of the equipment tools used and the working space of cold laboratory when firn core samples are mechanically prepared. In addition, the meltwater from discrete samples is liable to be contaminated during the experimental procedures, set for the analysis of ions using the standard IC system [18].

### 3.5. Application of the IC-melter

As an application of the IC-melter, we present measurement results of firn core sections between 20.11 and 22.85 m (approximately 1922 to 1934 CE) with depth resolution of  $\sim 1.8$  cm and an example along with a brief interpretation (Figs. 3 and S8). The calculation methods for the relative contributions of ss-Na<sup>+</sup>, nss-Ca<sup>2+</sup>, nss-SO<sub>4</sub><sup>2-</sup>, and H<sup>+</sup> contribution to theoretical EC (EC<sub>H+</sub>) of the meltwater are described in detail in Supplementary Material S3.

Continuous profiles presented in Figs. 3 and S8 show successful determination of major ions, in particular F<sup>-</sup> and CH<sub>3</sub>SO<sub>3</sub><sup>-</sup>, using the IC-melter. The high depth resolution data obtained allowed ion spikes

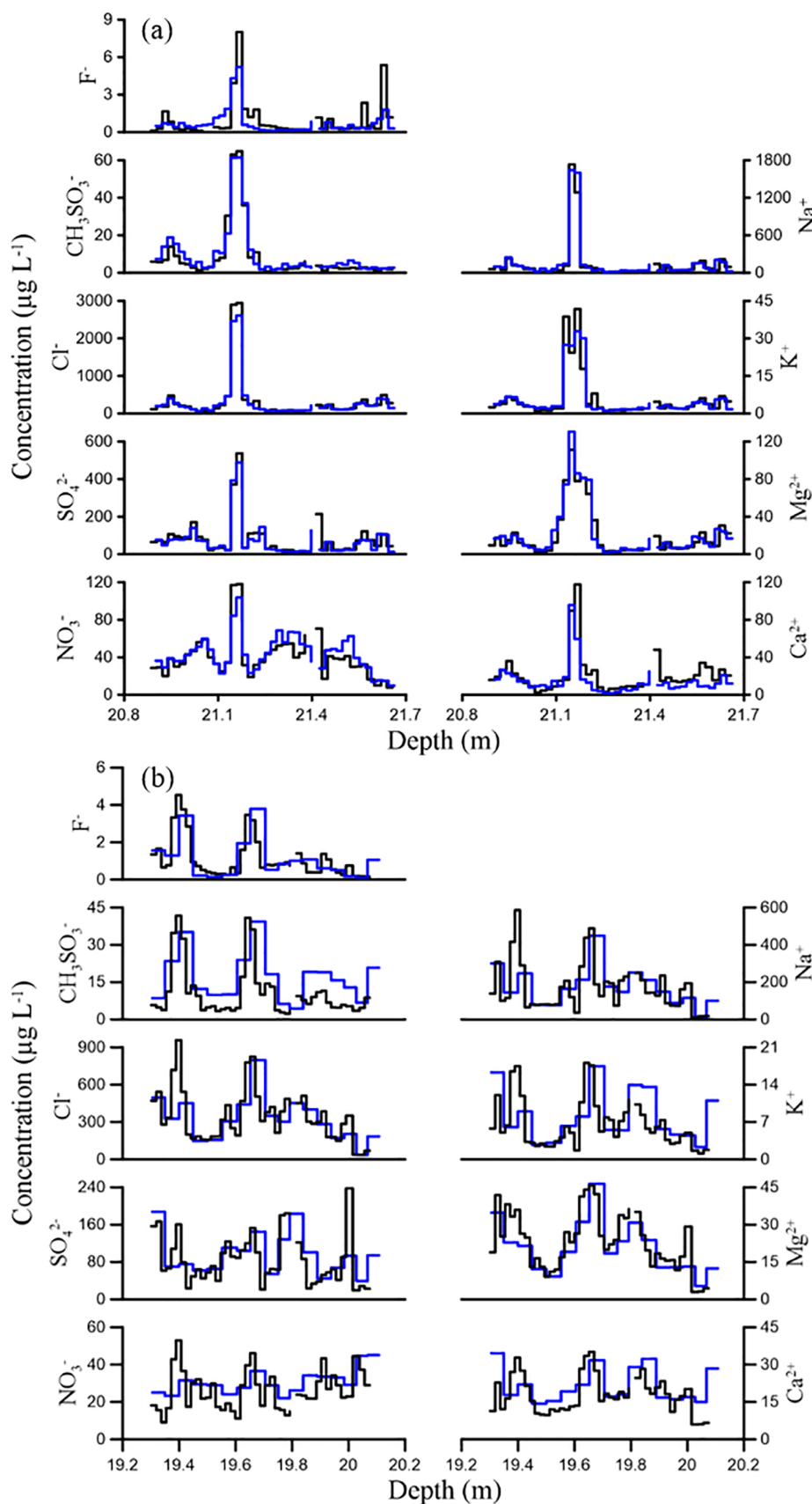


**Fig. 2.** (a) Reproducibility test for  $\text{F}^-$ ,  $\text{CH}_3\text{SO}_3^-$ ,  $\text{Cl}^-$ ,  $\text{SO}_4^{2-}$ ,  $\text{NO}_3^-$ ,  $\text{Na}^+$ ,  $\text{K}^+$ ,  $\text{Mg}^{2+}$  and  $\text{Ca}^{2+}$  by analyzing a sample of Styx-M core (black line) and turned upside-down sample of the original (blue line) (depth interval: 20.89–21.64 m deep). The discontinuous depth of the original sample and the turned upside down sample is about 21.38–21.41 m and 21.40–21.42 m, respectively. (b) Intercomparison of  $\text{F}^-$ ,  $\text{CH}_3\text{SO}_3^-$ ,  $\text{Cl}^-$ ,  $\text{SO}_4^{2-}$ ,  $\text{NO}_3^-$ ,  $\text{Na}^+$ ,  $\text{K}^+$ ,  $\text{Mg}^{2+}$  and  $\text{Ca}^{2+}$  in Styx-M core measured from our IC-melter system (black line) and conventional chiseling method (blue line) (depth interval: 19.30–20.07 m deep). (For interpretation of the references to colour in this figure legend, the reader is referred to the web version of this article.)

above background concentrations to be detected even in very thin layers. Several peaks ( $>$  mean value  $+1$  standard deviation (sd)) of  $F^-$  ( $>$   $\sim 2.0 \mu\text{g L}^{-1}$ ) or  $\text{CH}_3\text{SO}_3^-$  ( $>$   $\sim 16.0 \mu\text{g L}^{-1}$ ) were readily observed. A prominent feature was present at the depth of  $\sim 21.50$  m, where  $\text{ss-Na}^+$ ,  $\text{nss-Ca}^{2+}$ , and  $\text{CH}_3\text{SO}_3^-$  concentrations sourced from sea spray, crustal dust, and biogenic emissions had their highest values;  $F^-$  also showed its highest concentration. These results might have been related to abrupt changes in atmospheric composition that occurred during a transient event. Therefore, these spikes could be used to more accurately reconstruct oceanic and atmospheric events that occurred over a short time period in the past, if these signals are not strongly affected by post-depositional processes.

Annual layers were identified from variations in  $\text{ss-Na}^+$ ,  $\text{nss-SO}_4^{2-}$ ,  $\text{SO}_4^{2-}/\text{Na}^+$ ,  $\text{Cl}^-/\text{Na}^+$ , and  $\text{EC}_{\text{H+}}$ .  $\text{SO}_4^{2-}$  and  $\text{Na}^+$  were the key ions used for annual layer identification because their seasonal variations were generally well preserved in the context of post-depositional alteration, despite the low snow accumulation rate. In general, winter layers are enriched in  $\text{ss-Na}^+$  due to the extension of sea ice (an important source of sea spray) during winter [33]. The peaks of  $\text{nss-SO}_4^{2-}$  and  $\text{SO}_4^{2-}/\text{Na}^+$  can be used as proxies for summer layers because  $\text{SO}_4^{2-}$  inputs from emission sources other than sea spray increase the  $\text{nss-SO}_4^{2-}$  concentration, thus raising  $\text{SO}_4^{2-}/\text{Na}^+$  above the ratio of seawater ( $\sim 0.25$  w/w). This  $\text{nss-SO}_4^{2-}$  is primarily attributable to enhanced marine biogenic activity during the austral summer [6]. Local

or global volcanic events can temporarily disturb these trends. Ratios of  $\text{Cl}^-/\text{Na}^+$  greater than the seawater ratio ( $\sim 1.80$  w/w) were also used to designate summer layers [34].

Fig. 3 shows that clear summer layers could be identified for 14 years with one additional ambiguous layer. The annual accumulation rate in terms of water equivalent (w.e.) calculated from the peaks of the clear summer layers varied from 5.55 to 22.59 cm (average: 13.64 cm, sd: 4.74 cm), which is comparable to the value derived from the firn densification model (0.13 m w.e.) of Han et al. [29].

It is exhibited that the concentrations of  $\text{ss-Na}^+$  and  $\text{nss-Ca}^{2+}$ , which are primarily sourced from sea spray and terrestrial particles, respectively, were generally higher in winter (Fig. 3). Interestingly,  $F^-$  and  $\text{CH}_3\text{SO}_3^-$  showed also higher concentrations during winter; moreover,  $\text{ss-Na}^+$  covaried well with both  $F^-$  ( $r = 0.70$ ,  $p < 0.01$ ) and  $\text{CH}_3\text{SO}_3^-$  ( $r = 0.81$ ,  $p < 0.01$ ).

Despite the coherent seasonal variations, sea spray and terrestrial particles were not the main sources of  $F^-$  due to enrichment factors of  $F^-$  with respect to the seawater  $F/\text{Na}$  ratio ( $\sim 0.00012$  w/w) and the upper crust  $F/\text{Ca}$  ratio ( $\sim 0.012$  w/w), with values that were clearly higher than unity at the depths of episodic  $F^-$  peaks. When these ratios were considered, sea spray and terrestrial particles contributed only  $2.3 \pm 2.4\%$  (sd) and  $33.2 \pm 25.7\%$  of  $F^-$ , respectively. The  $F^-$  concentration ( $0.83 \pm 1.21 \mu\text{g L}^{-1}$ ) was several fold higher than the Antarctic background level ( $0.19 \mu\text{g L}^{-1}$ ) [35]. Therefore, emission

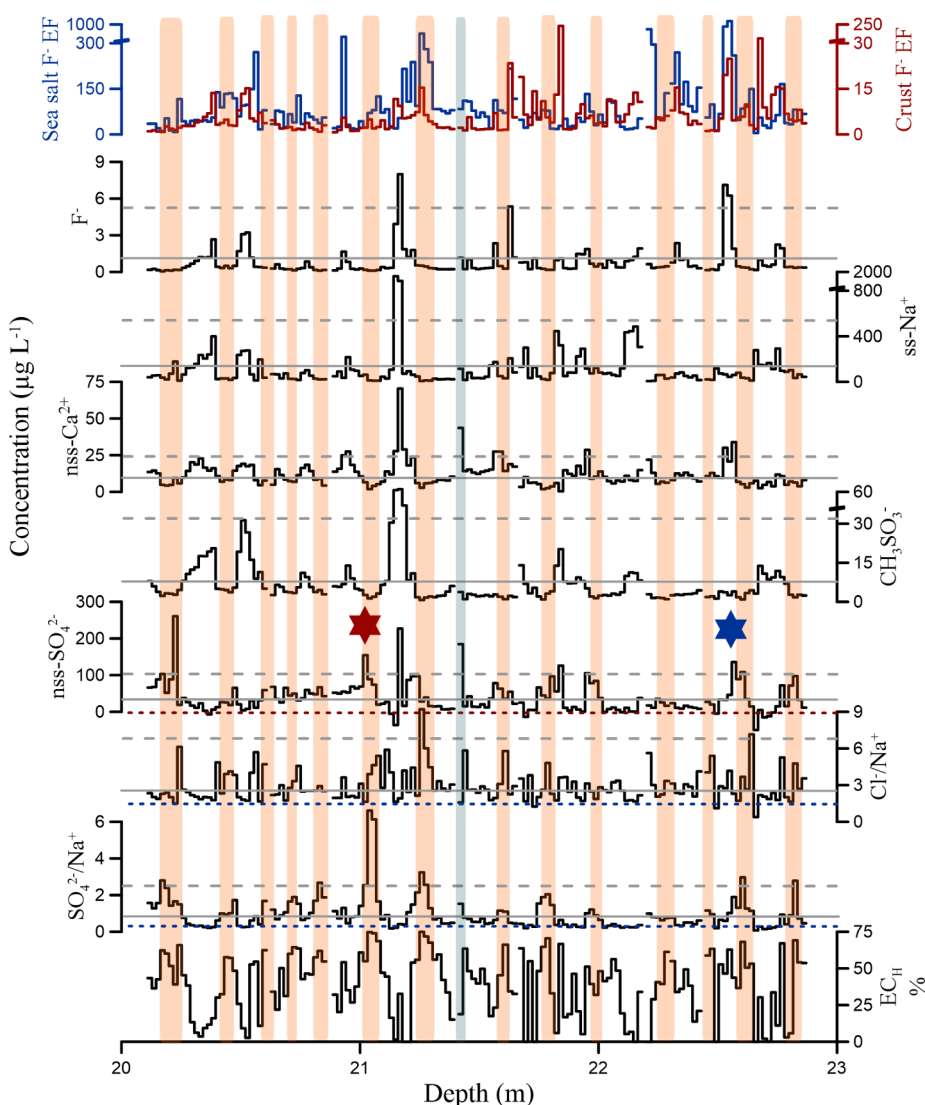


**Fig. 3.** The profiles of  $F^-$  EFs,  $F^-$ ,  $\text{ss-Na}^+$ ,  $\text{nss-Ca}^{2+}$ ,  $\text{CH}_3\text{SO}_3^-$ ,  $\text{nss-SO}_4^{2-}$ ,  $\text{Cl}^-/\text{Na}^+$ ,  $\text{SO}_4^{2-}/\text{Na}^+$ , and  $\text{EC}_{\text{H+}}$  in Styx-M core obtained using our IC-melter system (depth interval: 20.11–22.85 m deep;  $\sim 1936$ –1920 CE). The enrichment factors of  $F^-$  with respect to  $\text{Na}^+$  of seawater and  $\text{Ca}^{2+}$  of upper crust are presented as Sea salt  $F^-$  EF (blue line) and Crust  $F^-$  EF (red line), respectively, at the top of this figure. The vertical orange fields and green field indicate clear annual summer layers and ambiguous summer layer, respectively. The red and blue stars indicate the estimated global and Antarctic volcano eruption signals, assumed from  $\text{nss-SO}_4^{2-}$  and  $F^-$  profiles, respectively. The grey linear and dot lines on each species indicate its mean value and mean plus standard deviation value of Styx-M core, respectively. The red dot line on  $\text{nss-SO}_4^{2-}$  profile indicates the background level of  $\text{nss-SO}_4^{2-}$ . The blue dot lines on  $\text{Cl}^-/\text{Na}^+$  and  $\text{SO}_4^{2-}/\text{Na}^+$  profiles indicate  $\text{Cl}^-/\text{Na}^+$  (1.80 w/w) and  $\text{SO}_4^{2-}/\text{Na}^+$  (0.25 w/w) ratios of seawater, respectively. (For interpretation of the references to colour in this figure legend, the reader is referred to the web version of this article.)

sources other than sea spray and the crust were presumed to elevate  $F^-$  concentrations in Styx Glacier. Severi et al. [7] indicated that volcanic emissions are an important  $F^-$  source. Regional volcanic activities can contribute to higher  $F^-$  concentrations compared to other sites in Antarctica, but explanations other than temporal changes in emission intensity may be required to explain the annual cycle of  $F^-$ . Regarding the high  $F^-$  concentration in winter, it is necessary to consider the stability of  $F^-$  in sea spray and snowpack. Gaseous HF emitted from regional volcanoes can be efficiently adsorbed into sea spray (mainly in coastal areas) and crustal particles in the atmosphere under nearly neutral conditions during winter and in the less acidic winter layers of snowpack. In contrast, because the dissociation constant ( $6.3 \times 10^{-4} \text{ mol}^2 \text{ L}^{-2}$ ) of HF is much smaller than that of  $\text{H}_2\text{SO}_4$  (regarded as infinite), adsorption of HF into acidic summer sea spray is highly unlikely. Previous studies have reported exchange reactions of anions from sea spray, as  $\text{H}_2\text{SO}_4$  is adsorbed onto sea spray particles during summer and causes the release of gaseous HCl. Therefore, HF is unlikely to be stabilized through salt formation in the snow layer under the acidic conditions of summer; the  $F^-$  concentration might be low in that season. This process suggests that variations in  $F^-$  concentration might be closely related to the variability of sea spray during winter and presence of acidic species during summer.

$\text{CH}_3\text{SO}_3^-$  generally exhibits higher concentrations in the snow layer during summer, because it is an oxidation product of marine biogenically produced dimethylsulfide gas in the atmosphere. As expected, variations of  $\text{CH}_3\text{SO}_3^-$  in the snow pit sample from Styx Glacier generally indicated higher concentrations during summer and clearly before winter [30]. However, Fig. 3 shows that the concentration variations of  $\text{CH}_3\text{SO}_3^-$ , with higher levels during winter, markedly differed from those of surface snow on Styx Glacier. Previous studies have shown that the movement of  $\text{CH}_3\text{SO}_3^-$  from summer to the following winter layer can occur in firn core sections from sites with relatively low accumulation rates, such as Dolleman Island ( $\sim 0.34 \text{ m w.e.}$ ), Berkner Island ( $\sim 0.20 \text{ m w.e.}$ ), and Siple Dome ( $\sim 0.15 \text{ m w.e.}$ ) [26,36,37]. As a result, the covariance of  $\text{CH}_3\text{SO}_3^-$  and  $\text{ss-Na}^+$  suggests MSA migration may occur from the late summer layer to the winter layer, where  $\text{ss-Na}^+$  has a higher concentration.

Finally, two volcanic signals (one regarded as unknown global volcano ( $\sim 1930 \text{ CE}$ ) and one as unknown Antarctic volcano ( $\sim 1920 \text{ CE}$ )) were suggested based on the variations of  $\text{nss-SO}_4^{2-}$ ,  $F^-$ , and  $\text{SO}_4^{2-}/\text{Na}^+$ . The  $\text{SO}_4^{2-}/\text{Na}^+$  ratio at a depth of  $\sim 21.00 \text{ m}$  approached  $\sim 6$ , which is two-fold greater than the typical ratio of  $\text{SO}_4^{2-}/\text{Na}^+$ , over several years. Notably, the  $\text{nss-SO}_4^{2-}$  concentration showed a spike of  $\sim 150 \mu\text{g L}^{-1}$ , which was approximately twofold greater than the reference value ( $\sim 85 \mu\text{g L}^{-1}$ ); it then steadily decreased for  $\sim 2\text{--}3$  years. Furthermore,  $\text{nss-SO}_4^{2-}$  exhibited concentrations higher than background values (red dotted line in Fig. 3) during the following winter. This pattern of  $\text{nss-SO}_4^{2-}$  occurred at a depth of  $\sim 7.50 \text{ m}$  in the Styx-M core, which represented the Pinatubo eruption, as well as in snow layers deposited in Antarctica during global volcanic events [38]. As expected,  $\text{EC}_{\text{H}^+}$  showed trends similar to those of  $\text{nss-SO}_4^{2-}$ , indicating an increase in  $\text{H}_2\text{SO}_4$ .

$F^-$  concentrations were expected to be higher than average at other depth intervals due to the strength of emissions from volcanoes; however, they remained low, from  $\sim 0.12$  to  $1.66 \mu\text{g L}^{-1}$  during winter, in the depth interval of interest. HF can be transported to the polar region, in case it is injected into the stratosphere by volcanic eruptions. However, the transport efficiency of HF to the stratosphere might be much lower than that of  $\text{SO}_2$  because the Henry constant ( $130 \text{ mol m}^{-2} \text{ Pa}^{-1}$ ) of HF is  $\sim 10^4$ -fold greater than that of  $\text{SO}_2$  ( $0.012\text{--}0.014 \text{ mol m}^{-2} \text{ Pa}^{-1}$ ). Therefore, most HF can be removed through the wet deposition process in clouds during its entry into the atmosphere. Other possible mechanism is that, when HF was transported and deposited in the snow layer, it could be emitted out from the snow because of consistent acidity of the snow layer for a few years after volcanic eruptions, as we pointed out.

At the depth of  $\sim 22.50 \text{ m}$ , an episodic peak ( $\sim 7 \mu\text{g L}^{-1}$ ) of  $F^-$  was observed with low  $\text{ss-Na}^+$  and moderate  $\text{nss-Ca}^{2+}$  levels during winter, which markedly differed from their covariance pattern among depth intervals. Enrichment factors of  $F^-$  with respect to seawater and crustal composition approached 1000 and 20, respectively, indicating substantial inputs of additional  $F^-$ . Notably, although  $\text{nss-SO}_4^{2-}$  concentrations were relatively high ( $\sim 135 \mu\text{g L}^{-1}$ ) during summer, they decreased steadily and approached background levels during the following winter. This trend also clearly differed from the concentration trend of  $\text{nss-SO}_4^{2-}$  estimated at the depth of  $\sim 21.00 \text{ m}$  from unknown global volcanic events and thus may have represented degassing from local volcanoes in Victoria Land over a short time period. Although these high-resolution data of  $F^-$  might be helpful for identification of estimated volcanic signals, comprehensive interpretation of multiple volcanic proxies such as bismuth (Bi), thallium (Tl), and lead (Pb) isotopes should be carried out to clarify them.

#### 4. Conclusions

The coupling of multiple IC instruments and a firn core melter was successfully performed to provide with characteristics of high-resolution ion data of approximately  $1.8 \text{ cm}$  and processing speeds of  $1.1\text{--}1.7 \text{ h per } \sim 0.7\text{--}0.8 \text{ m firn core}$ .

To measure the target ions (i.e.,  $F^-$ ,  $\text{CH}_3\text{SO}_3^-$ ,  $\text{Cl}^-$ ,  $\text{NO}_3^-$ ,  $\text{SO}_4^{2-}$ ,  $\text{Na}^+$ ,  $\text{NH}_4^+$ ,  $\text{K}^+$ ,  $\text{Mg}^{2+}$ , and  $\text{Ca}^{2+}$ ), Thermo Fisher Scientific Dionex IonPac AS15-5  $\mu\text{m}$  ( $3 \times 150 \text{ mm}$ ) and CS12A-5  $\mu\text{m}$  ( $3 \times 150 \text{ mm}$ ) analytical columns were installed in the multi-IC system connected to the firn core melter. In particular,  $F^-$  and  $\text{CH}_3\text{SO}_3^-$  in a firn core from Antarctica were determined simultaneously and continuously for the first time using the on-line injection IC-melter.

Performance analysis of the IC-melter on a firn core section of the Styx-M core revealed the reliability of ion data from the IC-melter constructed in this study. This method might be suitable for detection of ionic species in Antarctic firn cores, thereby providing high-resolution ion data for reconstruction of rapid environmental changes that appear for only a short period of time; such signals are typically lost in averaged data that are obtained using the conventional method. This study demonstrated the usefulness of high-resolution ion detection by the improved IC-melter for estimation of ion seasonality, thus identifying annual layers and detecting probable volcanic signals in Antarctic firn cores.

However, as refinements of our method, the MDL ( $\sim 3.0 \mu\text{g L}^{-1}$ ) of  $\text{SO}_4^{2-}$  was generally greater than the MDLs of other IC-melters reported previously except for those from Severi et al. [15] due to a lack of baseline separation between  $\text{CO}_3^{2-}$  and  $\text{SO}_4^{2-}$ , although  $\text{SO}_4^{2-}$  was quantitatively determined in most samples in this study. Therefore, a CRD can be used to reduce the MDL of  $\text{SO}_4^{2-}$ . Also, the gradient elution method can be applied to enhance separation of  $\text{CO}_3^{2-}$  and  $\text{SO}_4^{2-}$ , although it should be carefully operated than the isocratic method. Unexpectedly, the neighboring peaks of  $\text{Na}^+$  and  $\text{NH}_4^+$  were not sufficiently separated in many samples, whereas they were in standard solutions. Because the concentration ratio of  $\text{Na}^+$  to  $\text{NH}_4^+$  in melted samples obtained from coastal areas of Antarctica is generally high,  $\text{NH}_4^+$  should be carefully determined the IC system with a short running time, which is usually deployed to the on-line IC-melter.

#### Declaration of Competing Interest

The authors declare that they have no known competing financial interests or personal relationships that could have appeared to influence the work reported in this paper.

#### Acknowledgements

This research was partly supported by Korea Polar Research Institute (KOPRI), South Korea, research grant (PE20190). This work

was also supported by the Basic Science Research Program through the National Research Foundation of Korea (NRF), South Korea, funded by the Ministry of Education, Science and Technology (NRF-2018R1A2B2006489), South Korea. We sincerely thank summer season researchers to take part in field activities at Styx Glacier on December, 2014.

## Appendix A. Supplementary data

Supplementary data to this article can be found online at <https://doi.org/10.1016/j.microc.2020.105377>.

## References

- [1] J. Jouzel, V. Masson-Delmotte, Paleoclimates: what do we learn from deep ice cores? *WIREs Clim. Change* 1 (2010) 654–669, <https://doi.org/10.1002/wcc.72>.
- [2] W. Dansgaard, Stable isotopes in precipitation, *Tellus* 16 (1964) 436–468, <https://doi.org/10.3402/tellusa.v16i4.8993>.
- [3] R.J. Delmas, Environmental information from ice cores, *Rev. Geophys.* 30 (1) (1992) 1–21, <https://doi.org/10.1029/91RG02725>.
- [4] M. Legrand, P.A. Mayewski, Glaciochemistry of polar ice cores: a review, *Rev. Geophys.* 35 (3) (1997) 219–243, <https://doi.org/10.1029/96RG03527>.
- [5] T. Kellerhals, L. Tobler, S. Brutsch, M. Sigl, L. Wacker, H. Gaggeler, M. Schwikowski, Thallium as a tracer for preindustrial volcanic eruptions in an ice core from Illimani, Bolivia, *Environ. Sci. Technol.* 44 (2010) 888–893, <https://doi.org/10.1021/es902492n>.
- [6] N.J. Abram, E.W. Wolff, M.A.J. Curran, A review of sea ice proxy information from polar ice cores, *Quat. Sci. Rev.* 79 (2013) 168–183, <https://doi.org/10.1016/j.quascirev.2013.01.011>.
- [7] M. Severi, S. Becagli, D. Frosini, M. Marconi, R. Traversi, R. Udisti, A novel fast ion chromatographic method for the analysis of fluoride in Antarctic snow and ice, *Environ. Sci. Technol.* 48 (2014) 1795–1802, <https://doi.org/10.1021/es404126z>.
- [8] P.R. Haddad, P.N. Nesterenko, W. Buchberger, Recent developments and emerging directions in ion chromatography, *J. Chromatogr. A* 1184 (2008) 456–473, <https://doi.org/10.1016/j.chroma.2007.10.022>.
- [9] E. Sanz Rodriguez, P.R. Haddad, B. Paull, Essential role of ion chromatography in constructing ice core paleoclimatic records, *Chromatography Today* (2015) 48–51.
- [10] A. Sigg, K. Fuhrer, M. Anklin, T. Staffelbach, D. Zurmühle, A continuous analysis technique for trace species in ice cores, *Environ. Sci. Technol.* 28 (2) (1994) 204–209, <https://doi.org/10.1021/es00051a004>.
- [11] R. Udisti, S. Becagli, E. Castellano, R. Mulvaney, J. Schwander, S. Torcini, E.W. Wolff, Holocene electrical and chemical measurements from the EPICA-Dome C ice core, *Ann. Glaciol.* 30 (2000) 20–26, <https://doi.org/10.3189/172756400781820750>.
- [12] R. Traversi, S. Becagli, E. Castellano, A. Migliori, M. Severi, R. Udisti, High-resolution fast ion chromatography (FIC) measurements of chloride, nitrate and sulphate along the EPICA Dome C ice core, *Ann. Glaciol.* 35 (2002) 291–298, <https://doi.org/10.3189/172756402781816564>.
- [13] T.M. Huber, M. Schwikowski, H.W. Gaggeler, Continuous melting and ion chromatographic analyses of ice cores, *J. Chromatogr. A* 920 (2001) 193–200, [https://doi.org/10.1016/S0021-9673\(01\)00613-6](https://doi.org/10.1016/S0021-9673(01)00613-6).
- [14] J. Cole-Dai, D.M. Budner, D.G. Ferris, High speed, high resolution, and continuous chemical analysis of ice cores using a melter and ion chromatography, *Environ. Sci. Technol.* 40 (2006) 6764–6769, <https://doi.org/10.1021/es061188a>.
- [15] M. Severi, S. Becagli, R. Traversi, R. Udisti, Recovering Paleo-records from Antarctic ice-cores by coupling a continuous melting device and fast ion chromatography, *Anal. Chem.* 87 (2015) 11441–11447, <https://doi.org/10.1021/acs.analchem.5b02961>.
- [16] E.C. Osterberg, M.J. Handley, S.B. Sneed, P.A. Mayewski, K.J. Kreutz, Continuous ice core melter system with discrete sampling for major ion, trace element, and stable isotope analyses, *Environ. Sci. Technol.* 40 (2006) 3355–3361, <https://doi.org/10.1021/es052536w>.
- [17] A. Morganti, S. Becagli, E. Castellano, M. Severi, R. Traversi, R. Udisti, An improved flow analysis-ion chromatography method for determination of cationic and anionic species at trace levels in Antarctic ice cores, *Anal. Chim. Acta* 603 (2007) 190–198, <https://doi.org/10.1016/j.aca.2007.09.050>.
- [18] S.-B. Hong, K. Lee, S.-D. Hur, S. Hong, T.-O. Soyol-Erdene, S.-M. Kim, J.-W. Chung, S.-J. Jun, C.-H. Kang, Development of melting system for measurement of trace elements and ions in ice core, *Bull. Korean Chem. Soc.* 36 (4) (2015) 1065–1081, <https://doi.org/10.1002/bkcs.10198>.
- [19] N.A.N. Bertler, P.J. Barrett, P.A. Mayewski, R.L. Fogt, K.J. Kreutz, J. Shulmeister, El Niño suppresses Antarctic warming, *Geophys. Res. Lett.* 31 (2004) L15207, <https://doi.org/10.1029/2004GL020749>.
- [20] N.A.N. Bertler, T.R. Naish, P.A. Mayewski, P.J. Barrett, Opposing oceanic and atmospheric ENSO influences on the Ross Sea region Antarctica, *Adv. Geosci.* 6 (2006) 83–86.
- [21] S. Becagli, E. Castellano, O. Cerri, M. Curran, M. Frezzotti, F. Marino, A. Morganti, M. Proposito, M. Severi, R. Traversi, R. Udisti, Methanesulphonic acid (MSA) stratigraphy from a Talos Dome ice core as a tool in depicting sea ice changes and southern atmospheric circulation over the previous 140 years, *Atmos. Environ.* 43 (2009) 1051–1058, <https://doi.org/10.1016/j.atmosenv.2008.11.015>.
- [22] M. Severi, S. Becagli, E. Castellano, A. Morganti, R. Traversi, R. Udisti, Thirty years of snow deposition at Talos Dome (Northern Victoria Land, East Antarctica): Chemical profiles and climatic implications, *Microchem. J.* 92 (2009) 15–20, <https://doi.org/10.1016/j.microc.2008.08.004>.
- [23] J.H.J. Coggins, A.J. McDonald, The influence of the Amundsen Sea Low on the winds in the Ross Sea and surroundings: Insights from a synoptic climatology, *J. Geophys. Res. Atmos.* 120 (2015) 2167–2189, <https://doi.org/10.1002/2014JD022830>.
- [24] S.-B. Hong, S.-J. Jun, K. Lee, J. Moon, C. Chang, S.D. Hur, S. Hong, Improvement and performance testing of melting system for measurement of trace elements in firn core drilled at NEMM site Greenland, *Int. J. Environ. Anal. Chem.* 98 (8) (2018) 725–742, <https://doi.org/10.1080/03067319.2018.1502282>.
- [25] W.I. Chang, J.H. Choi, S.B. Hong, J.H. Lee, Simultaneous measurements of gaseous nitrous acid and particulate nitrite using diffusion scrubber/steam chamber/luminol chemiluminescence, *Bull. Korean Chem. Soc.* 29 (8) (2008) 1525–1532, <https://doi.org/10.5012/bkcs.2008.29.8.1525>.
- [26] K.J. Kreutz, P.A. Mayewski, S.I. Whitlow, M.S. Twickler, Limited migration of soluble ionic species in a Siple dome Antarctica, ice core, *Ann. Glaciol.* 27 (1998) 371–377, <https://doi.org/10.3189/1998AOG27-1-371-377>.
- [27] R. Udisti, Multiparametric approach for chemical dating of snow layers from Antarctica, *Int. J. Environ. Anal. Chem.* 63 (3) (1996) 225–244, <https://doi.org/10.1080/03067319608026268>.
- [28] B. Stenni, F. Serra, M. Frezzotti, V. Maggi, R. Traversi, S. Becagli, R. Udisti, Snow accumulation rates in northern Victoria Land, Antarctica, by firn-core analysis, *J. Glaciol.* 46 (155) (2000) 541–552, <https://doi.org/10.3189/172756500781832774>.
- [29] Y. Han, S.-J. Jun, M. Miyahara, H.-G. Lee, J. Ahn, J.W. Chung, S.D. Hur, S.B. Hong, Shallow ice-core drilling on Styx glacier, northern Victoria Land, Antarctica in the 2014–2015 summer, *Jgsk* 51 (3) (2015) 343, <https://doi.org/10.14770/jgsk.2015.51.3.343>.
- [30] H. Kwak, J.-H. Kang, S.-B. Hong, J. Lee, C. Chang, S.D. Hur, S. Hong, A study on high-resolution seasonal variations of major ionic species in recent snow near the Antarctic Jang Bogo Station, *Ocean Polar Res.* 37 (2) (2015) 127–140, <https://doi.org/10.4217/OPR.2015.37.2.127> (in Korean).
- [31] E. Sanz Rodriguez, S. Poynter, M. Curran, P.H. Haddad, R.A. Shellie, P.N. Nesterenko, B. Paull, Capillary ion chromatography with on-column focusing for ultra-trace analysis of methanesulphonate and inorganic anions in limited volume Antarctic ice core samples, *J. Chromatogr. A* (1409 (2015b)) 182–188, <https://doi.org/10.1016/j.chroma.2015.07.034>.
- [32] Thermo Fisher Scientific USA, Product manual for Dionex IonPac CS12A and CG12A columns (Document NO 031132-09). <https://assets.thermofisher.com/TFS-Assets/CMD/manuals/4340-Man-031132-09-IonPac-CS12A-May10.pdf>, 2010.
- [33] X. Yang, J.A. Pyle, R.A. Cox, Sea salt aerosol production and bromine release: Role of snow on sea ice, *Geophys. Res. Lett.* 35 (2008) L16815, <https://doi.org/10.1029/2008GL034536>.
- [34] M.R. Legrand, R.J. Delmas, The ionic balance of Antarctic snow: A 10-year detailed record, *Atmospheric Environ.* 18 (9) (1984) 1867–1874, [https://doi.org/10.1016/0004-6981\(84\)90363-9](https://doi.org/10.1016/0004-6981(84)90363-9).
- [35] C. Saigne, S. Kirchner, M. Legrand, Ion-chromatographic measurements of ammonium fluoride, acetate, formate and methanesulphonate ions at very low levels in Antarctic ice, *Anal. Chim. Acta* 203 (1987) 11–21, [https://doi.org/10.1016/0003-2670\(87\)90003-1](https://doi.org/10.1016/0003-2670(87)90003-1).
- [36] E.C. Pasteur, R. Mulvaney, Migration of methane sulphonate in Antarctic firn and ice, *J. Geophys. Res.* 105 (D9) (2000) 11525–11534, <https://doi.org/10.1029/2000JD900006>.
- [37] M.A.J. Curran, A.S. Palmer, T.D. van Ommen, V.I. Morgan, K.L. Phillips, A.J. McMorris, P.A. Mayewski, Post-depositional movement of methanesulphonic acid at Law Dome, Antarctica, and the influence of accumulation rate, *Ann. Glaciol.* 35 (2002) 333–339, <https://doi.org/10.3189/172756402781816528>.
- [38] J. Cole-Dai, E. Mosley-Thompson, L.G. Thompson, Quantifying the Pinatubo volcanic signal in south polar snow, *Geophys. Res. Lett.* 24 (21) (1997) 2679–2682, <https://doi.org/10.1029/97GL02734>.